Electronic Supplementary Information

Multifunctional lanthanide MOFs with active sites as new platform for smart sensing of methylmalonic acid and anti-counterfeiting applications

Xiangmei Lu, Yue Tang, Guoping Yang* and Yao-Yu Wang

Key Laboratory of Synthetic and Natural Functional Molecule of the Ministry of Education, Shaanxi Key Laboratory of Physico-Inorganic Chemistry, Xi'an Key Laboratory of Functional Supramolecular Structure and Materials, College of Chemistry & Materials Science, Northwest University, Xi'an 710127, Shaanxi, P. R. China.

*Email: ygp@nwu.edu.cn

Materials and Instrumentations

All the reagents and solvents were purchased to use without further purification in the experiments. Infrared spectra were examined on Bruker EQUINOX-55 spectrophotometer in 4000−400 cm^{-1} (KBr pellets). Powder X-ray diffraction patterns were investigated through Bruker D8 ADVANCE X-ray powder diffractometer. Thermogravimetric analyses were tested on NETZSCH STA 449C microanalyzer (N_2 atmosphere, 10 °C min^{-1}). UV-vis spectra were measured on Hitachi U-3310 spectrometer. Luminescent spectra were determined on an Edinburgh FLS920 fluorescence spectrometer. The absolute quantum yields were tested on FluoroMax-4 spectrophotometer.

X-ray Crystal Structure Determination

The single-crystal X-ray diffractions were tested on Bruker SMART APEX II CCD diffractometer equipped with graphite monochromated Mo Kα radiation (λ = 0.71073 Å) *via* ϕ/ω scan method. The diffraction data were corrected for Lorentz and polarization effects for empirical absorption based on multiscan. The structures were solved by the direct methods and refined on F_2 *via SHELXTL* program. The anisotropic thermal parameters were applied to non-hydrogen atoms. The hydrogen atoms of ligands were calculated and added at ideal positions.

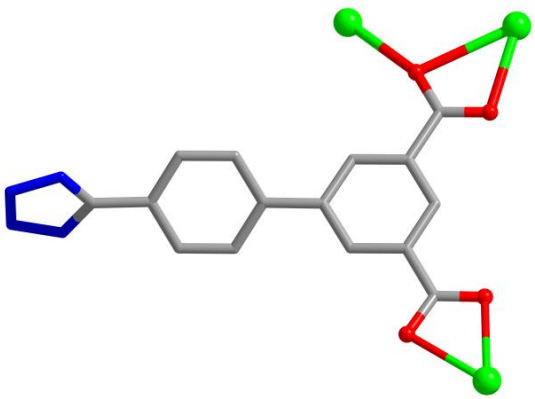

Fig. S1 The coordination modes of L^{3-} in **1-Eu**.

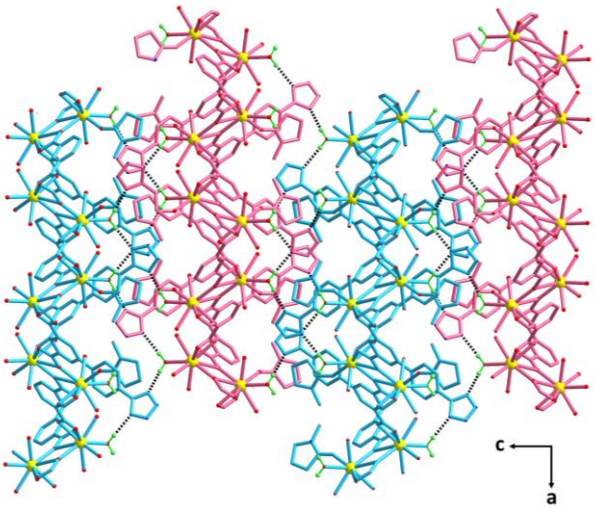

Fig. S2 The 3D framework of **1-Eu** along the *b* axis.

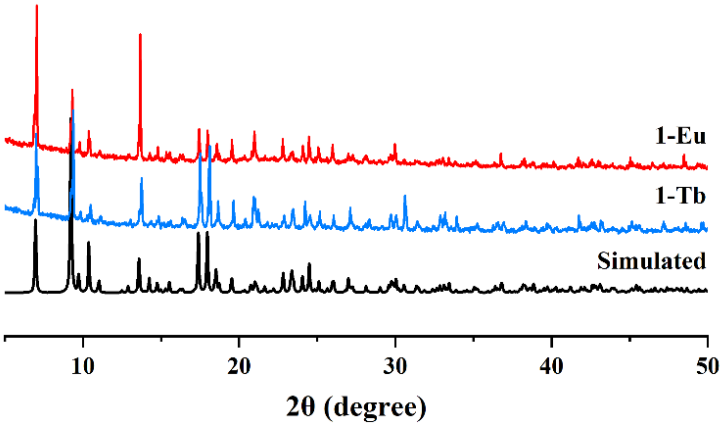

Fig. S3 PXRD patterns of **1-Eu** simulated from the X-ray single-crystal structure and as-synthesized samples of **1-Eu** and **1-Tb**.

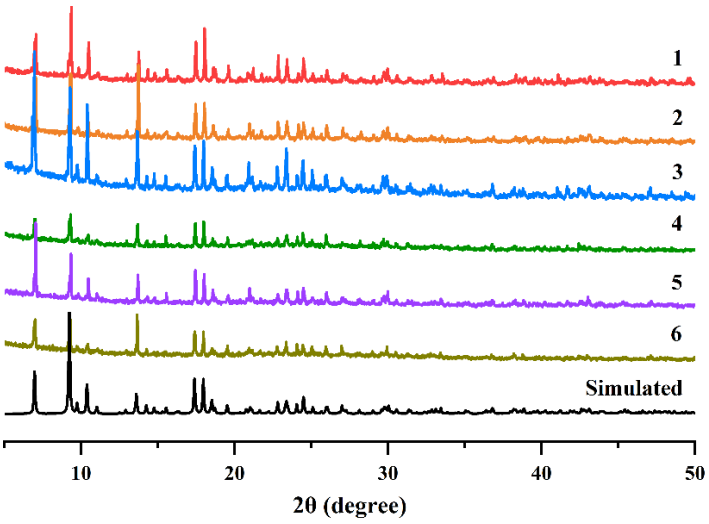

Fig. S4 PXRD patterns of doped samples.

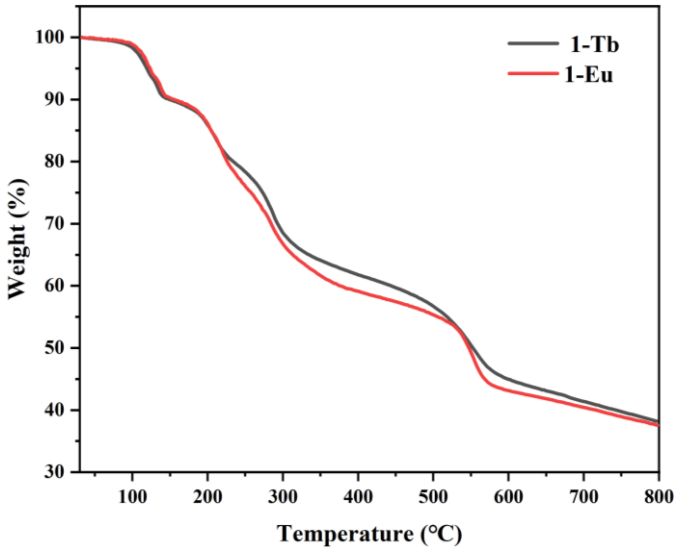

Fig. S5 The TGA plots of **1-Eu** and **1-Tb** under N_2 environment.

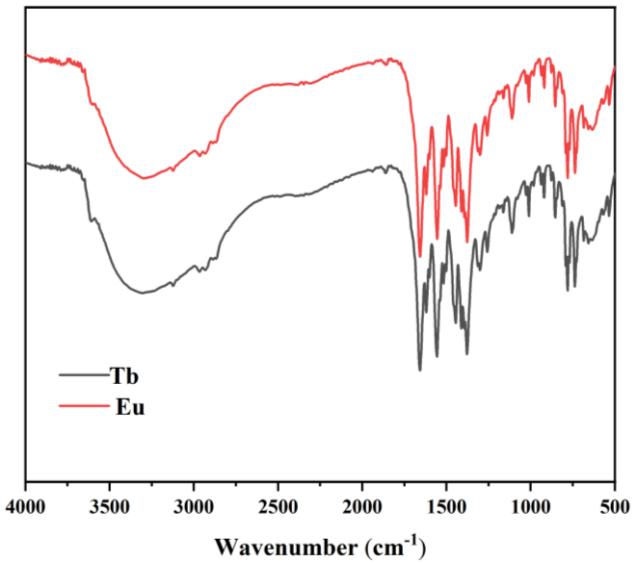

Fig. S6 The FT-IR spectra of **1-Eu** and **1-Tb**.

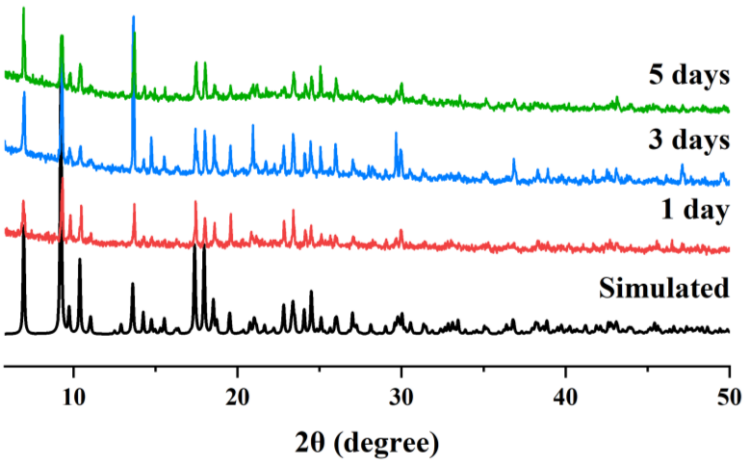

Fig. S7 PXRD of **1-Eu** after being immersed in the H_2O for 1-5 days.

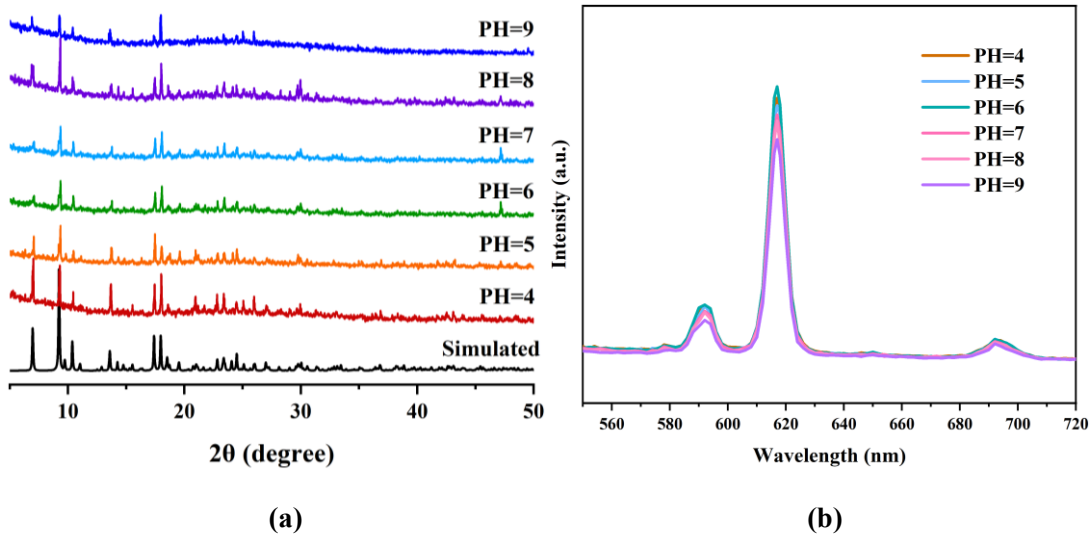

(a) **(b)**

Fig. S8 The PXRD patterns and luminescence spectra of **1-Eu** in different pH conditions.

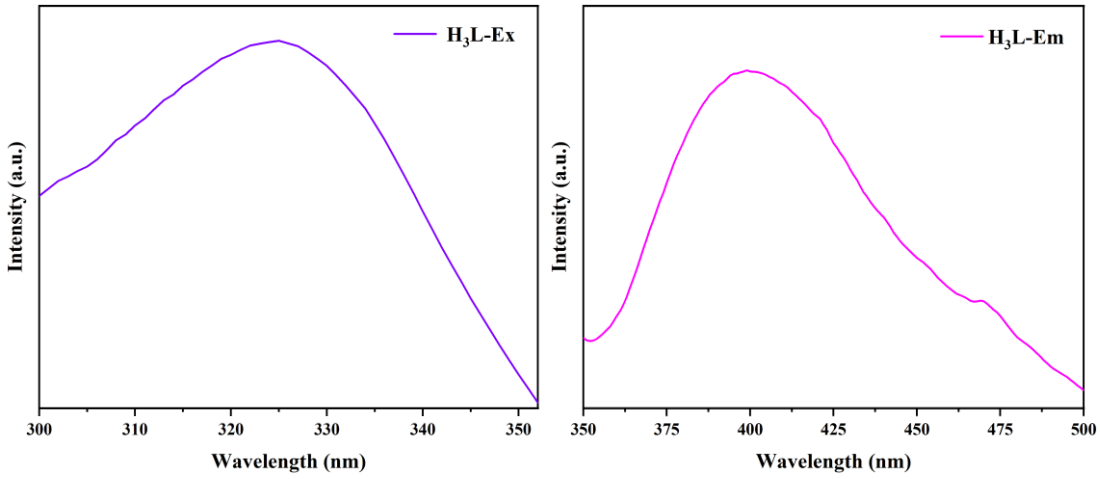

(a) **(b)**

Fig. S9 Excitation (a) and emission (b) spectra of H_3L (λ_{ex}=324 nm).

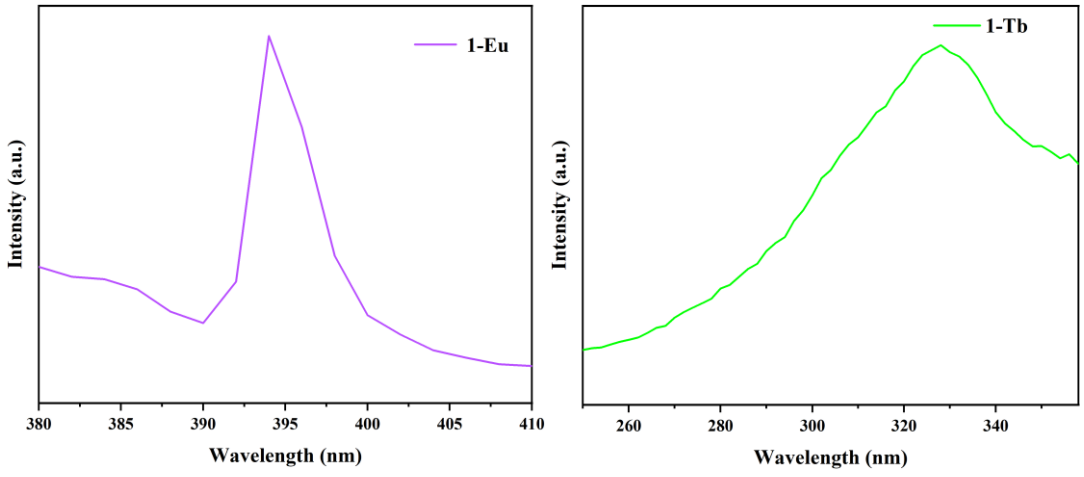

(a) **(b)**

Fig. S10 (a) Solid state excitation spectra of **1-Eu** (λ_{ex} = 394 nm) and (b) **1-Tb** (λ_{ex} = 330 nm).

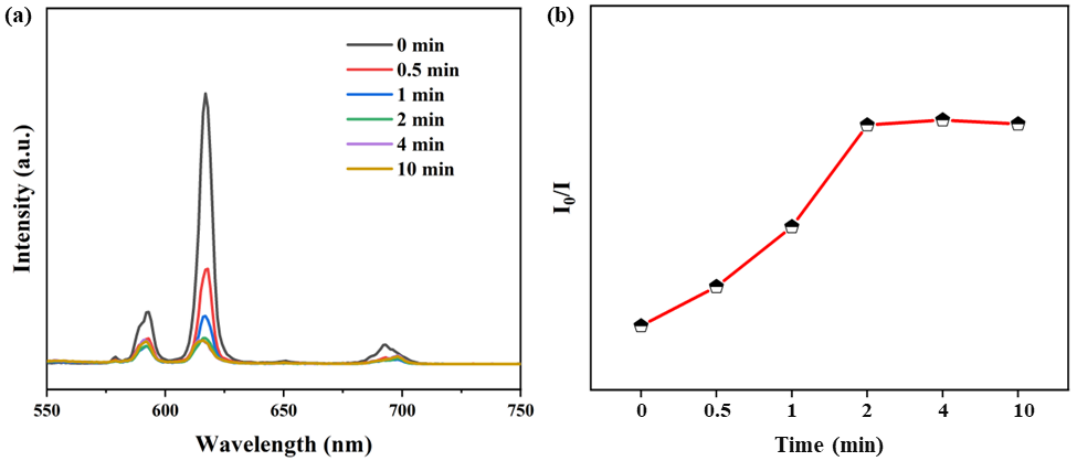

Fig. S11 (a) Variation of fluorescence intensity of **1-Eu** with different immersion time in MMA; (b) The corresponding line chart.

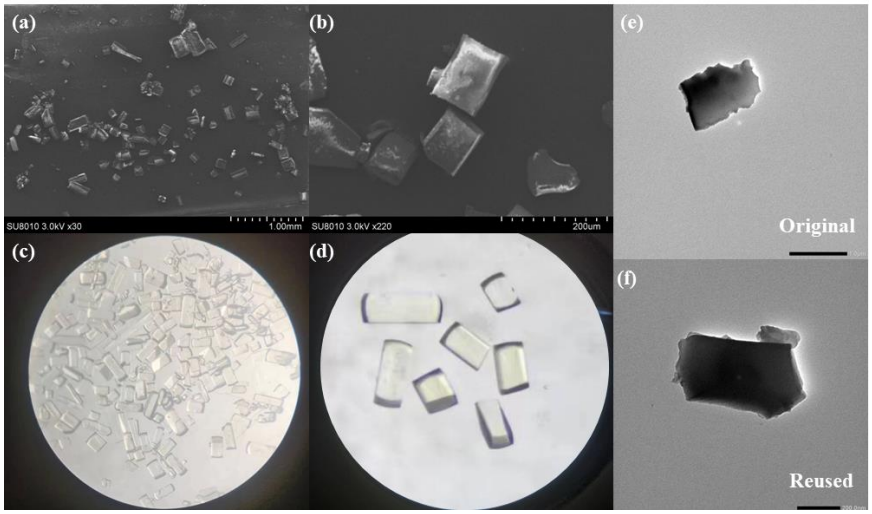

Fig. S12 The SEM images (a, b) and optical images (c, d) of **1-Eu**; The TEM images of the original (e) and reused (f) samples.

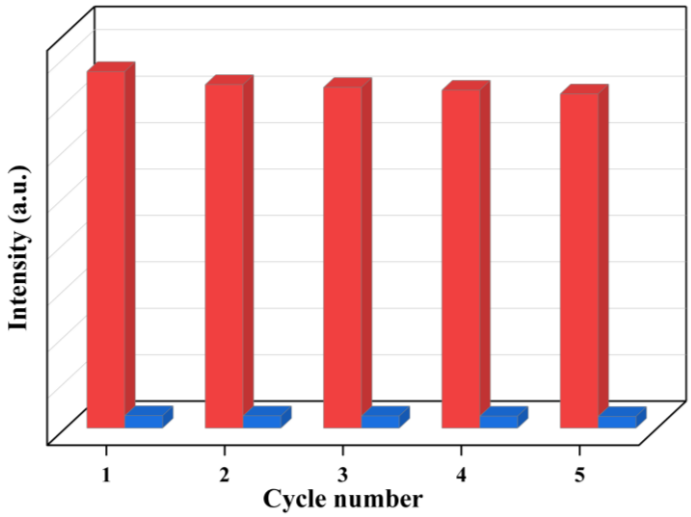

Fig. S13 Luminescence intensity of **1-Eu** adding MMA during recycle.

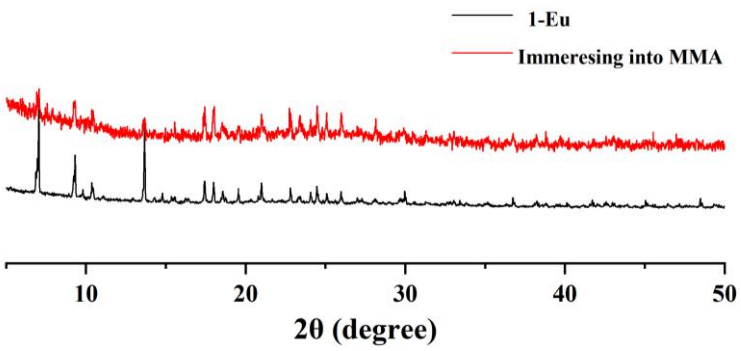

Fig. S14 PXRD patterns of **1-Eu** and **1-Eu** immersing into MMA.

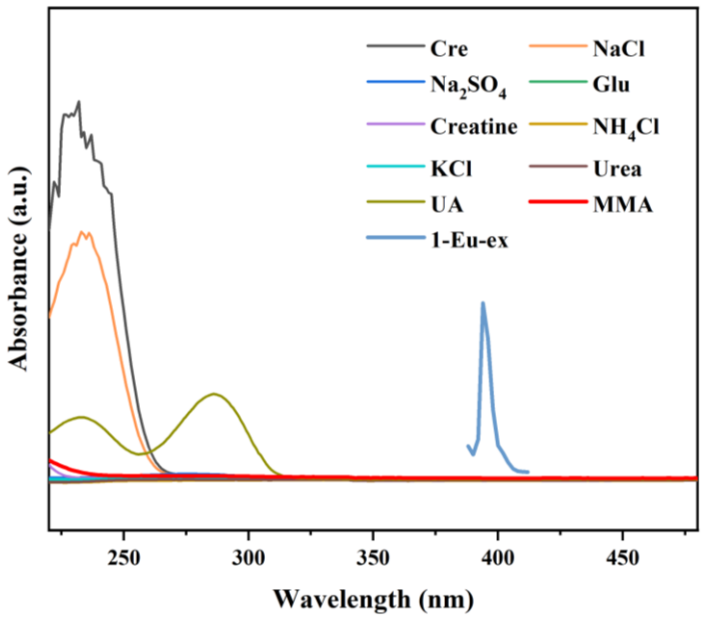

Fig. S15 UV-vis absorption spectra of Urea, Cre, NaCl, Glu, Na_2SO, UA, KCl, Creatine, NH_4Cl, MMA and the excitation spectrum of **1-Eu**.

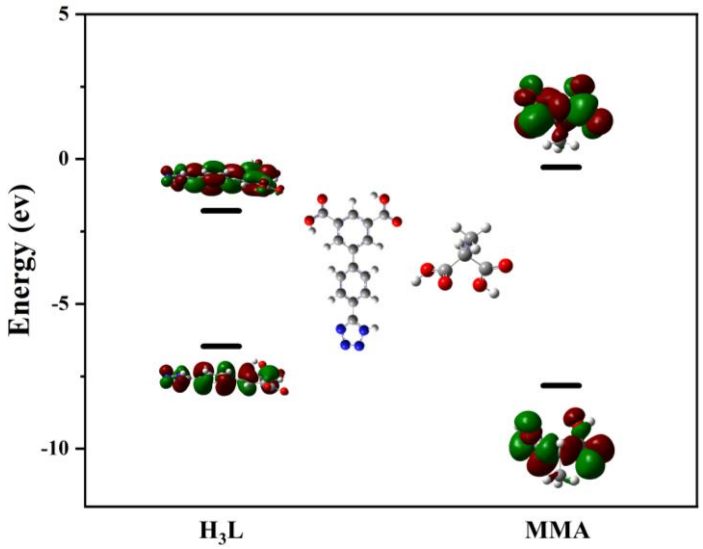

Fig. S16 Theoretical HOMO and LUMO for H_3L and MMA in water.

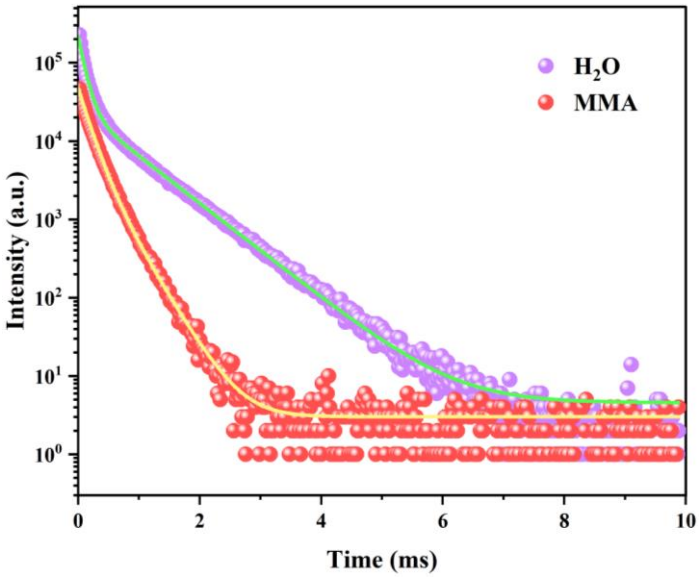

Fig. S17 Luminescence decay curves of **1-Eu** immersed in H_2O and MMA.

Table S1 Selected bond lengths (Å) and bond angles (°) for **1-Eu** and **1-Tb**.

1-Eu			
Eu(1)-O(4)#2	2.4740(18)	O(3)-Eu(1)-O(2)#1	115.26(6)
Eu(1)-O(5)#2	2.4779(18)	O(3)-Eu(1)-O(2)	50.37(6)
Eu(1)-O(2)	2.7196(18)	O(3)-Eu(1)-O(1)	94.16(7)
Eu(1)-O(2)#1	2.4651(18)	O(3)-Eu(1)-O(7)	81.16(7)
Eu(1)-O(3)	2.4051(18)	O(3)-Eu(1)-C(1)	24.62(7)
Eu(1)-O(1)	2.425(2)	O(1)-Eu(1)-Eu(1)#1	69.50(5)
Eu(1)-O(7)	2.433(2)	O(1)-Eu(1)-O(4)#2	138.94(7)
Eu(1)-O(6)	2.3555(19)	O(1)-Eu(1)-O(5)#2	140.79(6)
Eu(1)-O(8)	2.4937(19)	O(1)-Eu(1)-O(2)#1	74.12(7)
O(4)#2-Eu(1)-Eu(1)#1	100.56(4)	O(1)-Eu(1)-O(2)	71.79(6)
O(4)#2-Eu(1)-O(5)#2	52.77(6)	O(1)-Eu(1)-O(7)	138.65(7)
O(4)#2-Eu(1)-O(2)	120.22(6)	O(1)-Eu(1)-O(8)	70.66(7)
O(4)#2-Eu(1)-O(8)	128.71(6)	O(1)-Eu(1)-C(7)#2	149.56(7)
O(4)#2-Eu(1)-C(7)#2	26.12(6)	O(1)-Eu(1)-C(1)	81.89(7)
O(4)#2-Eu(1)-C(1)	127.10(7)	O(7)-Eu(1)-Eu(1)#1	147.64(6)
O(5)#2-Eu(1)-Eu(1)#1	71.41(4)	O(7)-Eu(1)-O(4)#2	68.54(7)
O(5)#2-Eu(1)-O(2)	73.34(6)	O(7)-Eu(1)-O(5)#2	78.35(7)
O(5)#2-Eu(1)-O(8)	138.46(7)	O(7)-Eu(1)-O(2)#1	144.58(6)
O(5)#2-Eu(1)-C(7)#2	26.68(7)	O(7)-Eu(1)-O(2)	127.84(7)
O(5)#2-Eu(1)-C(1)	74.34(6)	O(7)-Eu(1)-O(8)	68.56(7)

O(2)-Eu(1)-Eu(1)#1	31.12(4)	O(7)-Eu(1)-C(7)#2	70.49(7)
O(2)#1-Eu(1)-Eu(1)#1	34.77(4)	O(7)-Eu(1)-C(1)	104.48(8)
O(2)#1-Eu(1)-O(4)#2	76.61(6)	O(6)-Eu(1)-Eu(1)#1	118.65(5)
O(2)#1-Eu(1)-O(5)#2	75.72(6)	O(6)-Eu(1)-O(4)#2	76.03(7)
O(2)#1-Eu(1)-O(2)	65.89(6)	O(6)-Eu(1)-O(5)#2	128.47(6)
O(2)#1-Eu(1)-O(8)	144.19(6)	O(6)-Eu(1)-O(2)	142.37(7)
O(2)#1-Eu(1)-Eu(1)#1	34.77(4)	O(6)-Eu(1)-O(2)#1	88.45(7)
O(2)#1-Eu(1)-O(4)#2	76.61(6)	O(6)-Eu(1)-O(3)	150.59(7)
O(2)#1-Eu(1)-O(5)#2	75.72(6)	O(6)-Eu(1)-O(1)	75.03(7)
O(2)#1-Eu(1)-O(2)	65.89(6)	O(6)-Eu(1)-O(7)	89.13(8)
O(2)#1-Eu(1)-O(8)	144.19(6)	O(6)-Eu(1)-O(8)	76.57(7)
O(2)#1-Eu(1)-C(7)#2	75.52(7)	O(6)-Eu(1)-C(7)#2	102.09(7)
O(2)-Eu(1)-C(7)#2	97.64(6)	O(6)-Eu(1)-C(1)	156.07(7)
O(2)-Eu(1)-C(1)	25.78(6)	O(8)-Eu(1)-Eu(1)#1	130.63(5)
O(2)#1-Eu(1)-C(1)	91.31(7)	O(8)-Eu(1)-O(2)	107.89(6)
O(3)-Eu(1)-Eu(1)#1	80.98(4)	O(8)-Eu(1)-C(7)#2	139.03(7)
O(3)-Eu(1)-O(4)#2	124.44(6)	O(8)-Eu(1)-C(1)	90.00(7)
O(3)-Eu(1)-O(5)#2	76.76(6)		
1-Tb			
Tb(1)-O(4)#1	2.4571(15)	O(2)-Tb(1)-C(15)#1	101.38(6)
Tb(1)-O(3)#1	2.4507(15)	O(2)-Tb(1)-C(14)	24.45(6)
Tb(1)-O(1)	2.7615(16)	O(8)-Tb(1)-O(1)	108.50(6)
Tb(1)-O(1)#2	2.4325(16)	O(8)-Tb(1)-C(15)#1	138.83(6)
Tb(1)-O(2)	2.3699(16)	O(8)-Tb(1)-C(14)	90.46(6)
Tb(1)-O(8)	2.4724(17)	O(7)-Tb(1)-O(4)#1	68.76(6)
Tb(1)-O(7)	2.4044(18)	O(7)-Tb(1)-O(3)#1	78.31(6)
Tb(1)-O(6)	2.3292(17)	O(7)-Tb(1)-O(1)#2	145.02(6)
Tb(1)-O(5)	2.3962(18)	O(7)-Tb(1)-O(1)	127.21(7)
O(4)#1-Tb(1)-O(1)	120.44(5)	O(7)-Tb(1)-O(8)	68.33(6)
O(4)#1-Tb(1)-O(8)	128.01(6)	O(7)-Tb(1)-C(15)#1	70.54(6)
O(4)#1-Tb(1)-C(15)#1	26.35(6)	O(7)-Tb(1)-C(14)	104.20(7)
O(4)#1-Tb(1)-O(8)	128.01(6)	O(6)-Tb(1)-O(4)#1	75.97(6)
O(4)#1-Tb(1)-C(15)#1	26.35(6)	O(6)-Tb(1)-O(3)#1	128.75(6)
O(4)#1-Tb(1)-C(14)	127.70(6)	O(6)-Tb(1)-O(1)#2	87.78(6)
O(3)#1-Tb(1)-O(4)#1	53.24(5)	O(6)-Tb(1)-O(1)	141.57(6)
O(3)#1-Tb(1)-O(1)	73.03(5)	O(6)-Tb(1)-O(2)	150.70(6)
O(3)#1-Tb(1)-O(8)	138.71(6)	O(6)-Tb(1)-O(8)	76.51(6)

O(3)#1-Tb(1)-C(15)#1	26.93(6)	O(6)-Tb(1)-O(7)	90.59(7)
O(3)#1-Tb(1)-C(14)	74.46(5)	O(6)-Tb(1)-O(5)	75.53(6)
O(1)#2-Tb(1)-O(4)#1	76.98(5)	O(6)-Tb(1)-C(15)#1	102.22(6)
O(1)#2-Tb(1)-O(3)#1	75.68(5)	O(6)-Tb(1)-C(14)	155.26(6)
O(1)#2-Tb(1)-O(1)	65.66(6)	O(5)-Tb(1)-O(4)#1	139.74(6)
O(1)#2-Tb(1)-O(8)	144.08(6)	O(5)-Tb(1)-O(3)#1	139.94(5)
O(1)-Tb(1)-C(15)#1	97.60(6)	O(5)-Tb(1)-O(1)	70.87(5)
O(1)#2-Tb(1)-C(15)#1	75.69(6)	O(5)-Tb(1)-O(1)#2	74.09(6)
O(1)-Tb(1)-C(14)	25.58(6)	O(5)-Tb(1)-O(8)	70.79(6)
O(1)#2-Tb(1)-C(14)	90.96(6)	O(5)-Tb(1)-O(7)	138.86(6)
O(2)-Tb(1)-O(4)#1	125.36(6)	O(5)-Tb(1)-C(15)#1	149.75(6)
O(2)-Tb(1)-O(3)#1	77.21(5)	O(5)-Tb(1)-C(14)	80.36(6)
O(2)-Tb(1)-O(1)#2	114.84(5)	C(15)#1-Tb(1)-C(14)	101.38(6)
O(2)-Tb(1)-O(1)	49.99(5)	C(15)-O(4)-Tb(1)#3	92.99(13)
O(2)-Tb(1)-O(8)	74.30(6)	C(15)-O(3)-Tb(1)#3	92.64(13)
O(2)-Tb(1)-O(7)	81.15(7)	Tb(1)#2-O(1)-Tb(1)	114.34(6)
O(2)-Tb(1)-O(5)	92.33(6)		

Symmetry transformations used to generate equivalent atoms:

1-Eu: #1 -x+1,-y+1,-z+1; #2 -x+3/2,y+1/2,z; #3 -x+3/2,y-1/2,z. **1-Tb:** #1 -x+1/2,y+1/2,z; #2 -x+1,-y+1,-z+1; #3 -x+1/2,y-1/2,z; #4 x,-y+1/2,z-1/2; #5 x-1/2,-y+1/2,-z+1.

Table S2 HOMO and LUMO energies for H_3L and MMA.

Analytes	HOMO (eV)	LUMO (eV)	Band Gap (eV)
H_3L	**-6.46**	**-1.79**	**4.67**
MMA	**-7.82**	**-0.29**	**7.53**

Table S3 The luminescence decay times of **1-Eu** in H_2O and MMA.

Substance	Lifetimes (μs)
H_2O	**279.84 μs**
MMA	**121.55 μs**